

UCSF

UC San Francisco Electronic Theses and Dissertations

Title

Adaptation of the bone-PDL-cementum complex due to reduced functional loads in rats

Permalink

<https://escholarship.org/uc/item/5wv864g3>

Author

Niver, Eric L.

Publication Date

2011

Peer reviewed|Thesis/dissertation

Adaptation of the Bionic PDL-Cementum Complex Due to Reduced Functional Loads in Rats

by

Eric L. Noser

THESIS

Submitted in partial satisfaction of the requirements for the degree of

MASTER OF SCIENCE

in

Oral and Craniofacial Sciences

in the

GRADUATE DIVISION

ACKNOWLEDGEMENTS

It is my pleasure to recognize the tireless efforts of my research advisor, Dr. Sunita Ho, without whom this would not have been possible.

My sincere thanks are due to Dr. Mark Ryder and Dr. Stefan Habelitz, for serving on my thesis committee.

I would also like to thank the many people who contributed to this project: Janelle Greene, Dr. Ralf Peter Herber, Dr. Andrew Jang, Michael Kurylo, Narita Leong, Jeremy Lin, Dr. Mahesh Mankani, Grace Nonomura, and Linda Prentice for all their support and assistance. Additionally, the author thanks Dr. Peter Sargent, Department of Cell and Tissue Biology for the use of the ultramicrotome.

I gratefully acknowledge the funding sources that made this work possible: The Benjamin Dinstein Research Fund, UCSF; NIH/NIDCR R00 DE018212 (SPH), NIH/NCRR 1S10RR026645-01 (SPH); Strategic Opportunities Support (SOS) and T1 Catalyst Clinical and Translational Science Institute - CTSI University of California (SPH), San Francisco – UCSF, and Departments of Preventive and Restorative Dental Sciences, Orofacial Sciences, UCSF.

**Adaptation of the bone-PDL-cementum complex
due to reduced functional loads in rats**

Eric L. Niver

ABSTRACT

The aim of this study was to investigate the effect of reduced functional loads on the spatio-temporal changes in physico-chemical characteristics: structure, mineral composition, and mechanical properties of the bone-periodontal ligament-cementum complex using a rat model. In most vertebrate systems, mechanical loading of the dento-alveolar joint results in load-dependent adaptation of the hard (bone, cementum) and soft (periodontal ligament [PDL]) tissues of the joint and their interfaces. Within this load-mediated adaptation are load-independent changes due to innate physiological tooth drift. In order to investigate load-mediated effects due to reduced functional loads, two groups of six-week-old male Sprague-Dawley rats were fed nutritionally identical food in hard pellet (stiffness range: 127-158N/mm) or soft powder (stiffness range: 0.32-0.47N/mm) forms. Hard pellet food is the normal feed for rats. Temporal adaptation was mapped by identifying physico-chemical changes of the bone-PDL-cementum complex in rats of ages six, eight, twelve, and fifteen weeks. Spatial adaptation was mapped by identifying physico-chemical changes at the coronal, middle, and apical portions of the bone-PDL-cementum complex in rats. Adaptation of the bone-PDL-cementum complex due to reduced functional loads was identified by mapping changes in PDL-collagen orientation and birefringence using histochemistry and polarized light microscopy, bone and cementum morphology using micro X-ray computed tomography, mineralization of the PDL-cementum and PDL-bone interfaces by X-ray attenuation, and changes in microhardness of bone and cementum by microindentation.

Structurally altered PDL orientation, decreased PDL collagen birefringence, and decreased apical cementum resorption were observed with age. In addition, a gradual increase in X-ray attenuation, owing to mineral differences, was observed at the PDL-bone and PDL-cementum interfaces for both groups, but without significant differences in the gradients due to reduced functional loads. Reduced functional loads resulted in significantly ($p < 0.05$) lower microhardness of alveolar bone (0.93 ± 0.16 GPa) and secondary cementum (0.803 ± 0.13 GPa) compared to higher loads (1.10 ± 0.17 GPa and 0.940 ± 0.15 GPa respectively) at fifteen weeks. Based on the results from this study, occlusal loads differentially affect structural, compositional, and mechanical properties of local load-bearing sites of the bone-PDL-cementum complex, which could alter the overall biomechanical function of the dento-alveolar joint.

TABLE OF CONTENTS

Acknowledgements	iii
Abstract	iv
Table of Contents	vi
List of Figures	vii
Introduction	1
Materials and Methods	3
Results	7
Discussion	11
References	19
Figures	26

LIST OF FIGURES

Figure 1) Compression Testing System	26
Figure 2) 3D Reconstructions	28
Figure 3) Light Microscopy: Orientation	30
Figure 4) Virtual Histology: Resorption	32
Figure 5) Conventional Histology: Resorption	34
Figure 6) Interface Gradients	36
Figure 7) Microhardness	38
Figure 8) Schematic Force Diagram	40

1. INTRODUCTION

The unique anatomy of the dento-alveolar joint features two different hard tissues, cementum and alveolar bone, attached by the fibrous and vascularized periodontal ligament (PDL)¹. The general characteristics of cementum; a mineralized composite of fibrillar protein, apatite, and nonfibrillar protein, include a lamellar-like structure, with an inorganic range of 40-55% and organic range of 45-60%². Alveolar bone has a similar range of organic and inorganic material, however, the structure is very different from cementum. Alveolar bone is vascularized, and goes through physiological remodeling and significant response to mechanical loads identified as modeling of bone³.

The alveolar bone-PDL-tooth complex is a fibrous joint due to its dynamic nature, but unlike diarthroidal joints of the musculoskeletal system⁴, the dento-alveolar gomphosis joint has a limited range of motion⁵ during function. The load distribution on the dento-alveolar complex is facilitated in part by PDL-bone and PDL-cementum attachment sites, and the interfaces where the soft tissue (PDL) meets the hard tissues (bone and cementum) to jointly serve the common function of mechanical stress dissipation⁶ caused by dynamic loads. Over time, tissues, attachment sites, and interfaces adapt in ways identifiable by changes in physical and (bio)chemical properties in response to functional demands⁷ resulting in morphologically unique dental organs. Mechanical loading of the dento-alveolar complex causes localized biochemical changes, which in turn control resorption and apposition that allow macroscale structural changes⁸, a process which is fundamental to many aspects of dentistry, such as tooth eruption, orthodontic tooth movement, and tooth drift⁹. The intricate process of converting mechanical energy (i.e. functional loads on the occlusal surface) to chemical signals within the site-specific regions of the PDL-bone and PDL-cementum attachment

sites, identified as mechanobiology, is currently under investigation using various animal models^{10, 11}. Elucidating mechanobiology by investigating the related biochemical events at the tissue-level and correlating them to changes in structure, chemical composition, and mechanical properties in tissues and their interfaces would provide a better understanding of load-mediated adaptation of the 3D bone-PDL-tooth complex.

In order to investigate the load-mediated structural changes in human tissues and their interfaces, a systematic study using a rodent model is often employed. Previous studies^{12, 13} have shown that rats have a similar dental attachment apparatus as humans, and the tissues of the rat bone-PDL-cementum complex have been used to investigate load-mediated adaptation¹⁴⁻¹⁶. Load-mediated adaptation of the bone-PDL-tooth complex is investigated by changing the magnitude of occlusal loads using various models: hypo- and hyper-occlusion^{15, 17}, unopposed teeth¹⁸, orthodontic forces¹⁹, and soft and hard diets^{20, 21}. Changes in the magnitude of occlusal loads due to hypo-occlusion or substitution of a soft consistency diet reduces mechanical loading on molars¹⁴, resulting in load-mediated structural changes such as narrowed PDL space²², reduced volume, and reduced density of cortical and trabecular bone²³. In these studies, a confounding factor is physiological tooth drift, a well-documented phenomenon in both humans and rodents^{3, 24} that in and of itself could result in structural changes of the periodontal tissues. Irrespective of direction and magnitude of load, physiological tooth drift of rat molars in a distal direction is a constant^{25, 26}. Previous studies have identified localized mineral resorption and deposition, and altered mineral densities as drift-mediated adaptive structural changes of the bone-PDL-cementum complex^{12, 27}. Others have attributed altered glycosaminoglycan (GAG) levels and osteoclastic activity as drift-mediated adaptive changes at a cellular level²⁰. However, there have been no studies relating the influence of reduced functional loads coupled with natural tooth-drift on

adaptation of bone-PDL-cementum complex from a materials and mechanistic perspective.

The purpose of this study was to investigate adaptation of the bone-PDL-cementum complex due to reduced occlusal loads while taking into account the natural distal drift of molars in rats. In this study, the specific physico-chemical markers to identify spatiotemporal changes include: structure, mineral composition, and mechanical properties of tissues and their binding interfaces within the bone-PDL-cementum complex in rats.

2. MATERIALS AND METHODS

2.1. Animals and Experimental Diet

Fifty-six 6-week-old male Sprague-Dawley rats were obtained from Charles River Laboratories (Wilmington, MA) and housed at UCSF Animal Facilities. Animal housing, care, and euthanasia protocol complied with the guidelines of the Institutional Animal Care and Use Committee of UCSF and the National Institutes of Health. Rats were randomly allocated either to higher (N=32) or lower (N=24) functional load groups by feeding with either hard pellet or soft powder food. All groups were fed nutritionally identical food (PicoLab 5058, LabDiet, PMI), which was delivered in hard pellet form to the higher functional load group, and soft powder form to the lower functional load group. The rats were allowed food and water *ad libitum*. Time points were chosen to correspond with radiographic changes in bone mass and density and histologic changes in resorption activity reported by others in previous studies^{14, 18, 28, 29}. At the zero time point (age 6 weeks), eight rats (N=8) were sacrificed as controls, and considered to be in the higher functional load group as they are normally fed hard pellets from the time the pups are weaned. At the subsequent time points: age eight weeks, age twelve weeks,

and age fifteen weeks, eight rats (N=8) from each group were sacrificed, and their mandibles immediately harvested for specimen preparation.

2.2. Food Stiffness Testing

Nutritionally identical hard (pellet form) and soft (powder form) rodent food (PicoLab 5058, LabDiet, PMI) was collected from the UCSF Animal Facilities and mechanically tested to assess the stiffness properties. Stiffness is a mechanical property and is defined as the amount of force required to deform a material by one unit. Compression tests were conducted using a standard compression/tension materials testing system (Figure 1A, EnduraTec, Bose Electrofoce 3200 system, Minnetonka, MN) with 0.01mm and 0.1N displacement and load resolution, respectively, and 6.5mm and 50N maximum displacement range and load capacity, respectively. Determination of hard food stiffness was achieved by compressively loading individual unconfined pellets (Figure 1B) at a rate of 0.01mm/s to an average maximum load of 43.5N. Soft food stiffness was determined by conducting bulk confined compression tests (Figure 1C), within a half-filled plastic container. Soft food was loaded at a rate of 0.1mm/s to an average maximum displacement of 5.52mm. Soft food was loaded at a faster rate to avoid particle flow that may result from lower loading rates. Stiffness was determined by the slope of the linear portion of the load versus the displacement curve. Mean stiffness of hard food was 150 ± 15 N/mm. Mean stiffness of soft food was 0.4 ± 0.1 N/mm.

2.3. Deparaffinized Sections for Histology

The molar portions of the left half-mandibles (N=4) harvested at the different time points from each group were fixed in sodium phosphate-buffered (pH 7.0) 4% formaldehyde for 3 days. The specimens were demineralized by immersing in Immunocal (Decal Chemical Corporation, Tallman, NY) formic acid solution for 4

weeks³⁰. The specimens were considered decalcified when addition of saturated ammonium oxalate to the solution failed to produce a precipitate³¹.

The demineralized specimens were dehydrated using 80%, 95%, and 100% Flex alcohol (Richard-Allan Scientific, Kalamazoo, MI) and embedded in paraffin (Tissue Prep-II, Fisher Scientific, Fair Lawn, NJ). 5-6 μm thick sections from the paraffin block were taken using a rotary microtome (Reichert-Jung Biocut, Vienna, Austria) using disposable steel blades (TBF Inc., Shur/Sharp, Fisher Scientific, Fair Lawn, NJ). The paraffin serial sections were mounted on Superfrost Plus microscope slides (Fisher Scientific, Fair Lawn, NJ), deparaffinized with xylene then stained with either H&E or Picrosirius Red. The stained tissues were characterized for structural orientation and integration of the PDL with bone and cementum, using a light microscope (BX 51, Olympus America Inc., San Diego, CA) and analyzed using Image Pro Plus v6.0 software (Media Cybernetics Inc., Silver Springs, MD). Polarized light was used to create a contrast, and identify direction due to the natural birefringence of the collagen in alveolar bone, PDL and cementum.

2.4. Specimen Preparation for Micro X-Ray Computed Tomography (Micro XCT)

The molar portions of the left mandibles (N=4) from each group were fixed in sodium phosphate-buffered (pH 7.0) 4% formaldehyde for 3 days. All specimens were thoroughly rinsed, stored, and imaged in 70% ethanol. The tungsten anode setting was 75 keV with a power of 6W using a 4x magnification (Micro XCT, Xradia Inc., Concord, CA). Computed tomography (CT) was used to study the 3D structure of bone-PDL-cementum complex and allowed selection of virtual parallel slices spaced by 1 μm in different planes (Figure 2), thus illustrating the structure of tissues and their interfaces. Each specimen was scanned with identical experimental parameters, then reconstructed in 3D (Figure 2A) and viewed with identical contrast and brightness settings to identify

spatiotemporal trends in X-ray attenuation. The longitudinal sectioning planes in the buccal-lingual (coronal sections, Figure 2B) and mesial-distal (sagittal sections, Figure 2C) directions for each specimen was oriented to bisect the distal root of the second mandibular molar, as identified by the apical orifice, followed by serial virtual sectioning within 0.5mm. Additionally, using transverse sections from occlusal to apical regions of the distal root of the second molar (Figure 2D) for each specimen, twelve radial measurements were taken from the PDL space 80µm into both the alveolar bone and the secondary cementum at regular intervals around the perimeter of the root, and analyzed using ImageJ³² to plot intensity, which is representative of x-ray attenuation of alveolar bone and secondary cementum, as a function of distance from the PDL space.

2.5. Ultrasectioned specimens for microindentation

The molar portions of the right mandibles (N=4) were first sectioned mesio-distally to isolate the distal root of the second molar, then bucco-lingually to bisect the root using a diamond wafering blade and a low-speed saw (Isomet, Buehler, Lake Bluff, IL) under wet conditions. The specimens were glued to AFM steel stubs (Ted Pella, Inc., CA) using epoxy for ultrasectioning with an ultramicrotome. A diamond knife (MicroStar Technologies, Huntsville, TX) was used to perform final sectioning by removing 300nm thin sections³³. The sectioned surface of the remaining block was characterized using a light microscope. Ultrasectioning resulted in a relatively flat surface with low roughness permitting orthogonality between tip and specimen; a necessary criterion for indentation³³.

2.6. Microhardness of ultrasectioned specimens

Microindentation on mineralized tissues using ultrasectioned blocks (N=4) was performed under dry conditions with the use of a microindenter (Buehler Ltd., Lake Bluff,

IL) and a Knoop diamond indenter (Buehler Ltd., Lake Bluff, IL). Each specimen was indented in cementum and alveolar bone, with approximately 15 and 30 indents in each tissue. The distance between any two indents was chosen as per ASTM standard³⁴. Microindentation was performed using a normal load of 10g force, and the long diagonal of each indent was immediately measured with the use of a light microscope with Image-Pro data acquisition software (Media Cybernetics, Inc., Bethesda, MD). The Knoop microhardness (HK) values of respective regions were determined with the use of the following equation: $HK = (0.014229 \cdot P) / D^2$ where "P" is the normal load in Newtons (N) and "D" is the length of the long diagonal in millimeters (mm)³⁴. Statistically significant differences between groups were determined using Student's t-test with a 95% confidence interval.

3. RESULTS

The tissues of the bone-PDL-cementum complex in a rat mandible have a complex architecture, and the morphology of each molar (and the corresponding PDL and alveolar bone) is unique. The distal root of the 2nd mandibular molar, M2/D, is an ideal biomechanical model for the adaptive changes investigated in this study. For orientation, Figure 2 shows Micro XCT images of M2/D reconstructed in 3D, along with 2D slices through the root of M2/D. Results are divided into sections demonstrating that reduced mechanical loading caused: 1) changes in PDL collagen fiber organization; 2) altered spatial distribution of resorption in cementum; 3) altered spatial distribution of modeling in alveolar bone; 4) changes in mineralization of alveolar bone and cementum at the bone-PDL and PDL-cementum interfaces; 5) changes in the mechanical hardness of bone and cementum.

3.1. Changes in PDL collagen fiber organization

Light microscope images of M2 at 10x are shown in Figure 3, each with an inset illustrating the appearance of the bone-PDL-cementum complex in the apical region at the distal attachment sites using polarized light microscopy (PLM). Polarized microscopy of picosirius red stained sections of M2/D reveal distinct differences between the PDL collagen fibers with lower loads compared to higher loads. PDL collagen fibers subjected to lower loads were weakly birefringent (Figures 3A, 3B), with a disorganized, lower intensity, and patchy appearance, suggesting collagen degradation. PDL collagen fibers subjected to higher loads demonstrated demonstrate a strong birefringence (Figures 3C, 3D), with a well oriented, organized, and bright appearance, suggesting well-maintained collagen structure.

3.2. Altered distribution of cementum resorption

3D reconstructions of the M2/D region subjected to lower and higher occlusal loads demonstrate pitting on the distal root surface, characteristic of resorption activity at the PDL-cementum attachment site. Analysis of reconstructed 3D and 2D slices revealed a regional pattern of resorption in cementum. A representative 2D slice of M2/D shown in Figure 4A illustrates the affected regions: the coronal region (CR) in red with only primary cementum, the mid-root region (MR) in purple spanning the transition between primary and secondary cementum, and the apical region (AR) in blue with only secondary cementum.

Extensive resorption was observed in the CR and MR regions (Figure 4B, highlighted in red and purple respectively) at all time points in rats subjected to lower occlusal loads. Apposition of secondary cementum is seen with age as expected³⁵, but cementum resorption in the AR region decreased over time in rats subjected to lower occlusal loads.

In rats subjected to higher occlusal loads (Figure 4C), the distribution of cementum resorption in the CR and MR regions is similar at all time points to those subjected to lower occlusal loads. Also, secondary cementum apposition occurred with age. However, in contrast to those with lower occlusal loads, resorption in the AR region (highlighted in blue, Figure 4C) is markedly increased over time.

3.3. Altered distribution of alveolar bone modeling activity

Alveolar bone opposing resorbed cementum demonstrated cement (reversal) lines, characteristic of coincident modeling activity in bone. Analysis of H&E stained light microscope images of M2/D showed a distribution of cement lines (Figure 5) corresponding to regional patterns of cementum resorption identified in Figure 4. In rats subjected to lower occlusal loads (Figure 5B), cement lines in alveolar bone increase with age, especially in the CR region opposing areas of primary cementum resorption. In rats subjected to higher occlusal loads (Figure 5C), cement lines in alveolar bone increase with age, especially in the AR region opposing areas of secondary cementum resorption.

3.4. Mineral gradients at the PDL-alveolar bone and PDL-cementum interfaces

High-resolution tomography of the M2/D region revealed a gradient in X-ray attenuation of alveolar bone at the PDL-bone interface, and in the secondary cementum at the PDL-cementum interface, for both lower and higher occlusal loads all time points (Figure 6). Representative 3D reconstructions (Figure 6) demonstrate the anatomical locations along the M2/D root where the intensity gradients were measured on the 2D slices. For each 2D slice, the intensity at the PDL-bone and PDL-cementum interfaces was measured, and then plotted as a function of distance (Figure 6) from the PDL space. Measurements were made to avoid cortical bone and endosteal and/or other

vascular spaces. For the PDL-bone and PDL-secondary cementum interfaces, the intensity plots in Figure 6 consistently demonstrated a gradual increase in the first 25 μ m from the PDL space. The changes in intensity correspond to changes in X-ray attenuation due to variations in mineral content within the alveolar bone and secondary cementum. The results in Figure 6 show that the first 25 μ m near the PDL-bone and PDL-cementum attachment sites are less mineralized than the bulk tissues.

3.4. Mechanical properties of bulk secondary cementum and alveolar bone

The bulk tissue microhardness values were evaluated to distinguish significant differences between dissimilar tissues and changes within a tissue due to potential adaptation. Microhardness technique is not sensitive enough to detect heterogeneity within a tissue due to the size of the probe. Techniques such as nanoindentation should be implemented to identify tissue heterogeneity. Thus, care was taken to perform microindentation (Figure 7C) in bulk tissue, avoiding indentation at the edges.

Knoop hardness of bone increased with age, from 0.64 ± 0.14 GPa at 6 weeks to 1.1 ± 0.17 GPa in the higher load group and 0.93 ± 0.16 GPa in the lower load group at 15 weeks (Figure 7). An increasing trend in hardness was observed in bone in the bone-PDL-cementum complex subjected to higher occlusal loads compared to the lower occlusal load group at all experimental time points (8, 12, and 15 weeks). Additionally, bone subjected to higher occlusal loads was significantly harder ($p < 0.05$) at the 12-week (1.0 ± 0.19 GPa) and 15-week (1.1 ± 0.17 GPa) experimental time points than bone subjected to lower occlusal loads (0.89 ± 0.18 GPa and 0.93 ± 0.16 GPa respectively).

Knoop hardness of cementum also increased with age, from 0.51 ± 0.11 GPa at 6 weeks to 0.94 ± 0.15 GPa in the higher load group and 0.80 ± 0.13 GPa in the lower load group at 15 weeks (Figure 7). An increasing trend in hardness was observed in bone in the bone-PDL-cementum complex subjected to higher occlusal loads compared to the

lower occlusal load group at all experimental time points (8, 12, and 15 weeks). Additionally, bone subjected to higher occlusal loads was significantly harder ($p < 0.05$) at the 12-week (0.90 ± 0.15 GPa) and 15-week (0.94 ± 0.15 GPa) experimental time points than bone subjected to lower occlusal loads (0.78 ± 0.15 GPa and 0.80 ± 0.13 GPa respectively).

4. DISCUSSION

Functional loading on the bone-PDL-tooth complex of a molar is predominantly due to mastication of food. In addition to nutritional composition, the physical characteristics of food such as hardness, elasticity/plasticity, and particle size³⁶ change the magnitudes and velocities of masticatory forces, and thus are significant factors in modulating functional loads. In this study, modulation of functional load was accomplished by changing the hardness of nutritionally equivalent food³⁷: a hard pellet diet with a higher compressive strength, compared to a soft powder diet with negligible compressive strength. Consequently, in this study, rats on a hard pellet diet experienced higher functional loads, while those fed a soft, powdered diet experienced lower functional loads (Figure 1). Subsequently, adaptation due to higher and lower loads was investigated by spatial and temporal mapping of physico-chemical properties, which included structure, mineral gradients, and hardness changes of bone and cementum and their attachments sites, PDL-bone and PDL-cementum. Spatial and temporal changes in structure were evaluated using 2D reconstructed virtual slices from tomography, 3D reconstructed volumes, and conventional histology. Picrosirius red staining was used to enhance the innate collagen birefringence within tissues, a marker for collagen structural integrity. X-ray attenuation gradients of hard tissue directly adjacent (within $80\mu\text{m}$) to the PDL-bone and PDL-cementum attachment sites were

analyzed using the 2D reconstructed slices to identify relative changes in local mineral density. Temporal changes in microhardness of cementum and bone were used to identify changes in load-bearing characteristics.

It is known that the tissues of the rat bone-PDL-cementum complex have a complex architecture, and the morphology of each molar (and the corresponding PDL and alveolar bone) is unique, including an increased angulation of the distal roots of molars within the alveolus of the mandible and maxilla³⁸. Despite the inter-anatomic variation in physical characteristics of molars and the corresponding alveolar socket, innate adaptation on the mesial and distal sides of each root of each molar occurs due to distally directed tooth drift in rats³⁹. Innate distal root angulation compounded with distal drift⁴⁰ resulting in resorption of the cementum and adjacent bone on the distal side of all roots in rat molars⁴¹ was also reported when subjected to higher occlusal forces from a hard pellet diet¹⁶.

The data presented in this study focuses on the distal root of the second mandibular molar, M2/D (Figure 2) from both higher and lower occlusal load groups. Biomechanically, M2/D experiences occlusal-apical forces from functional loading, and mesial-distal forces from the 1st molar (M1) and the 3rd molar (M3). Hence, the compound effects of reduced masticatory forces, multi-directional forces from M1 and M3, and naturally occurring distal drift forces in rat molars can be investigated using the distal root of M2, the most biomechanically representative site in the area of interest. Specifically, the coronal, mid-root, and apical anatomical locations were chosen, as these are speculated to be the local weight-bearing sites along the root length, due to differences in PDL-orientation, cementum type, and observed spatial adaptations of the bone-PDL-cementum complex to date^{11, 42, 43}.

Identified structural changes in this study include 1) the loss of birefringence and directionality of PDL (Figure 3), and 2) varied cementum resorption (Figure 4) and

alveolar bone modeling (Figure 5) patterns in the coronal, middle, and apical regions of the root between experimental groups. The chain of events following the observed adaptation at the three potential load-bearing sites of the bone-PDL-cementum complex can be explained as follows:

The decreased magnitude of functional load using the soft, powdered diet could decrease the turnover rate of collagen in the PDL due to decreased tooth movement relative to bone⁴⁴. Constant PDL turnover rate is necessary to maintain its inherent structural and mechanical integrity. A decrease and/or loss of occlusal function demonstrated atrophy of the PDL, and was related to a loss in lower and higher molecular weight proteoglycans responsible for the structural maintenance and mechanical integrity of the PDL⁴⁵⁻⁵³. The innervated PDL contains vasculature, various types of collagen (including types I, III, V, VI, and XII) and several noncollagenous proteins that contribute to the chemically bound fluid, maintenance of hydrostatic pressure, and the load dissipating characteristics^{43, 54}. However, the PDL matrix is degraded when the PDL structure is broken down, including the molecular structure of collagen, as a result of decreased turnover due to inadequate loading^{11, 55}. A strong PDL birefringence was observed in all three anatomical locations of the complex subjected to higher loads (Figures 3C and 3D), while a patchy, diffuse birefringence was observed in PDL subjected to lower functional loads (Figures 3A and 3B). Fundamentally, enhancement of birefringence can only be observed when the picosirius red molecules are bound to oriented, highly organized collagen molecules⁵⁶. In comparison with the higher intensity birefringence of PDL, the lower intensity, diffuse birefringence can be related to degraded PDL in the bone-PDL-cementum complex due to lower occlusal loads. Aberrations to functional loads can change the physiological programming of the PDL cells, altering the biochemical events and changing the structural and mechanical

integrity of the PDL matrix, redefining the related local events of the bone-PDL-cementum complex and overall functional biomechanics.

Functional loads on the PDL are distributed from the coronal to the apical aspect of the bone-PDL-cementum complex^{42, 43, 57}. Based on current dogma, coronal, acellular, primary cementum is responsible for tooth attachment, while apical, cellular, secondary cementum is responsible for resisting functional loads⁵. The observed local changes in cementum, corresponding bone, and the PDL could be a necessary adaptive response to preserve the functional mechanics of the dento-alveolar joint, by forming local load-bearing sites within the bone-PDL-cementum complex of molar teeth.

Local load distribution sites are often broadly categorized as tension and compression sites due to widening and narrowing of the PDL-space within the bone-PDL-cementum complex⁵⁴. From a pure biomechanics perspective, the functional loads on a tooth define the 3D spatial relationship of the tooth with the alveolar bone and the resulting tension and compression sites in the complex. In this study, as lower loads decreased the PDL integrity and its load distributing characteristics, the mechanobiological events at the PDL-cementum and PDL-bone attachment sites were compromised, resulting in resorption of bone and primary cementum of the distal root. This observation was consistent, but to a lesser degree, within the bone-PDL-cementum complex subjected to higher loads. Rather, higher occlusal loads transmit greater force to the apical region of the root, and as a result increased secondary cementum resorption was observed. While secondary cementum resorption in teeth subjected to lower loads was observed at earlier time points, the resorption decreased over time (Figure 4B), indicating the effects of the reduced functional loads apically on the bone-PDL-cementum complex. Over time, reduced functional loads suppress activity of the masticatory muscles, decrease load across the facial skeleton, diminish apically directed compressive forces³⁶, and result in decreased secondary cementum resorption.

In a load-mediated bone-PDL-cementum complex, resorption sites in both humans and rats are a result of narrowed PDL-space in compression zones, while bone growth and cementum apposition are indicative of widened PDL-space in tension zones^{9, 18, 19}. In this study, resorption sites were consistently observed in the coronal, middle, and apical regions of the distal side of M2/D in six-week-old rats, considered to be subjected to higher occlusal loads. However, when subjected to lower loads over time, the degree of resorption and resorption patterns were altered at the load-bearing sites. This observation could be a result of adaptation of the bone-PDL-cementum complex that had been accustomed to higher loads, suddenly “forced” to accommodate a minimal load. Furthermore, the effects of reduced load are more evident with time, as changes in resorption patterns in the twelve- and fifteen-week groups (Figure 4B) are more distinct. Hence, these results can be considered necessary, local adaptations of the bone-PDL-cementum complex to accommodate decreased functional loads.

It should be noted that, common to both groups are resorption related events in cementum and bone due to distal drift of rat molars; an innate programmed event in rats. Accounting for the aforementioned loss in the structural integrity of PDL, adaptation due to innate distal drift of rat molars together with reduced functional loads should explain the temporal effects: 1) decreased coronal and apical resorption in bone-PDL-cementum complex subjected to higher loads, and 2) a decrease in apical resorption when subjected to lower loads.

Despite the consistent observation of resorption pits, a constant gradient in mineral profile was maintained both spatially and temporally (Figure 6) at the PDL-bone and PDL-cementum interfaces subjected to higher and lower functional loads. Physical and chemical gradients are naturally found between dissimilar materials in the structure of a load bearing tooth, such as enamel and dentin, and cementum and dentin⁵⁸⁻⁶⁰, where they are thought to distribute functional loads. This unique and well-defined

characteristic provides an optimum biomechanical function for a tooth by eliminating discontinuities within the system. Simultaneously, the PDL continues to experience forces due to tension and compression events at its attachment sites with bone and cementum. These mechanically related events modulate the biochemical expressions through site-specific cells, which act as transducers to increase or decrease expression of biomolecules that promote or inhibit biomineralization. In this study, higher loads resulted in increased hydrostatic pressure within the endosteal and trabecular spaces, resulting in adaptation of alveolar bone identified by reversal lines in Figure 5. Additionally, in regions of bone modeling activity subjected to higher loads, concentric cement lines were observed. Although not shown in detail here, these concentric lines bordered trabecular spaces or foramina in the alveolar bone, and in some cases the lines appeared to meet, closing the space completely^{55, 61-66}. At the later time points, less adaptation was observed in the bone-PDL-cementum complexes subjected to lower loads (Figures 4 and 5); however, no significant differences were observed in the mineral gradient at the PDL-bone and PDL-cementum interface sites (Figure 6). Some possible explanations for the lack of differences in mineral gradients between groups: 1) The lower magnification at which the mineral changes were documented was accurate only for macro-scale events, and not sensitive to the micro-scale events within the mineralized tissues. 2) In order to compare the gradient in cementum to that in alveolar bone, equal distances of 80 μm from the PDL attachment site into the respective hard tissues were measured. In the younger groups, the thin layer of secondary cementum limited mineral gradient measurements to the first 80 μm from the PDL-bone and PDL-cementum attachment sites, and thus this method could not detect any changes in the surrounding bone. 3) The reduction in functional loads could only have a moderate effect on bone and cementum mineral concentrations and may be confirmed by extending the study to later time points. Regardless, from a materials and mechanics

perspective, the locally identified gradual increase in mineral at the PDL-bone and PDL-cementum interfaces serves to accommodate functional loads.

Although no difference was observed in x-ray attenuation, a significant increase in the hardness values (Figure 7) of cementum and bone was observed with age in both groups. During development, an increase in hardness with age is expected within groups, however the significant increase in hardness between groups at the 12 and 15 week time points can be related to the maintenance of the 'quality' of bone and cementum. Functional mineralization is best understood by investigating load-resisting characteristics of composite matrices (like bone and cementum) while accounting for the interaction of mineral inside and outside the collagen fibrils that form the tissue scaffold⁶⁷. However, a compromised mineral-collagen interaction commonly observed in inadequately loaded mineralized tissue could compromise the overall 'quality' of the mineralized tissue⁶⁸. This could explain the significantly greater hardness (Figure 7) of bone and cementum subjected to higher loads when compared to inadequately loaded bone and cementum. Deviation from normal function changes the mechanical stress patterns within the bone-PDL-cementum complex at the local load-bearing sites of the PDL-bone and PDL-cementum interfaces; thus compromising mechanobiology and affecting modeling and remodeling related events⁵⁵ necessary to maintain optimum function.

Summarizing the observations of this study with a biomechanical model (Figure 8), the reduced functional loads can cause a decrease in tooth rotation, lateral loads, and different stress states within the bone-PDL-cementum complex. As with any multi-rooted tooth, the molar could pivot or rotate using the inter-radicular bone as a fulcrum⁵⁷, and alter localized widening and narrowing of the PDL-space. This in turn could result in altered tension and compression of the PDL at the PDL-bone and PDL-cementum attachment sites, and the observed patterns identified as adaptation.

In conclusion, diet consistency affects the functional occlusal loads experienced by the bone-PDL-cementum complex of the dento-alveolar joint. Lower forces may not be sufficient to maintain tissue homeostasis, and could precipitate degradation of collagen organization in the PDL, alter the distribution of stress-induced resorption, and result in lower 'quality' bone and cementum. From a clinical perspective, this study provides insights into modulation of load on the bone-PDL-cementum complex to improve tooth function impaired due to periodontal disease or non-physiological loads such as those involved in orthodontics and prosthodontics.

REFERENCES

1. Nanci A, Bosshardt DD. Structure of periodontal tissues in health and disease. *Periodontol 2000* 2006;40:11-28.
2. Bosshardt DD, Selvig KA. Dental cementum: the dynamic tissue covering of the root. *Periodontol 2000* 1997;13:41-75.
3. Saffar JL, Lasfargues JJ, Cherruau M. Alveolar bone and the alveolar process: the socket that is never stable. *Periodontol 2000* 1997;13:76-90.
4. Mow VC, Ratcliffe A, Poole AR. Cartilage and diarthrodial joints as paradigms for hierarchical materials and structures. *Biomaterials* 1992;13(2):67-97.
5. Nanci A. *Ten Cate's Oral Histology: Development, Structure, and Function*. 6th ed. Saint Louis: Mosby; 2003.
6. Benjamin M, Toumi H, Ralphs JR, Bydder G, Best TM, Milz S. Where tendons and ligaments meet bone: attachment sites ('entheses') in relation to exercise and/or mechanical load. *J Anat* 2006;208(4):471-90.
7. Frost HM. Wolff's Law and bone's structural adaptations to mechanical usage: an overview for clinicians. *Angle Orthod* 1994;64(3):175-88.
8. Frost HM. A 2003 update of bone physiology and Wolff's Law for clinicians. *Angle Orthod* 2004;74(1):3-15.
9. Wise GE, King GJ. Mechanisms of tooth eruption and orthodontic tooth movement. *J Dent Res* 2008;87(5):414-34.
10. Henneman S, Von den Hoff JW, Maltha JC. Mechanobiology of tooth movement. *Eur J Orthod* 2008;30(3):299-306.
11. Krishnan V, Davidovitch Z. On a path to unfolding the biological mechanisms of orthodontic tooth movement. *J Dent Res* 2009;88(7):597-608.

12. Page R, Schroeder E. Periodontitis in man and other animals. Basel: Karger; 1982.
13. Klausen B. Microbiological and immunological aspects of experimental periodontal disease in rats: a review article. *J Periodontol* 1991;62(1):59-73.
14. Tanaka E, Sano R, Kawai N, Langenbach GE, Brugman P, Tanne K, et al. Effect of food consistency on the degree of mineralization in the rat mandible. *Ann Biomed Eng* 2007;35(9):1617-21.
15. Ohshima S, Komatsu K, Yamane A, Chiba M. Prolonged effects of hypofunction on the mechanical strength of the periodontal ligament in rat mandibular molars. *Arch Oral Biol* 1991;36(12):905-11.
16. Mavropoulos A, Kiliaridis S, Bresin A, Ammann P. Effect of different masticatory functional and mechanical demands on the structural adaptation of the mandibular alveolar bone in young growing rats. *Bone* 2004;35(1):191-7.
17. Kumazawa M, Kohsaka T, Yamasaki M, Nakamura H, Kameyama Y. Effect of traumatic occlusion on periapical lesions in rats. *J Endod* 1995;21(7):372-5.
18. Bondevik O. Tissue changes in the rat molar periodontium following alteration of normal occlusal forces. *Eur J Orthod* 1984;6(3):205-12.
19. Nakamura Y, Noda K, Shimoda S, Oikawa T, Arai C, Nomura Y, et al. Time-lapse observation of rat periodontal ligament during function and tooth movement, using microcomputed tomography. *Eur J Orthod* 2008;30(3):320-6.
20. Kingsmill VJ, Boyde A, Davis GR, Howell PG, Rawlinson SC. Changes in bone mineral and matrix in response to a soft diet. *J Dent Res* 2010;89(5):510-4.
21. Grunheid T, Langenbach GE, Brugman P, Everts V, Zentner A. The masticatory system under varying functional load. Part 2: effect of reduced masticatory load on the degree and distribution of mineralization in the rabbit mandible. *Eur J Orthod* 2010.

22. ElDeeb ME, Andreasen JO. Histometric study of the effect of occlusal alteration on periodontal tissue healing after surgical injury. *Endod Dent Traumatol* 1991;7(4):158-63.
23. Bresin A, Kiliaridis S, Strid KG. Effect of masticatory function on the internal bone structure in the mandible of the growing rat. *Eur J Oral Sci* 1999;107(1):35-44.
24. Baron R, Tross R, Vignery A. Evidence of sequential remodeling in rat trabecular bone: morphology, dynamic histomorphometry, and changes during skeletal maturation. *Anat Rec* 1984;208(1):137-45.
25. Belting CM, Schour I, Weinmann JP, Shepro MJ. Age changes in the periodontal tissues of the rat molar. *J Dent Res* 1953;32(3):332-53.
26. Hardt AB. Bisphosphonate effects on alveolar bone during rat molar drifting. *J Dent Res* 1988;67(11):1430-3.
27. Sicher H, Weinmann, J.P. Bone Growth and Physiologic Tooth Movement. *Am. J. Orthodontics & Oral Surg* 1944;30:109.
28. Endo Y, Mizutani H, Yasue K, Senga K, Ueda M. Influence of food consistency and dental extractions on the rat mandibular condyle: a morphological, histological and immunohistochemical study. *J Craniomaxillofac Surg* 1998;26(3):185-90.
29. Kimura R, Anan H, Matsumoto A, Noda D, Maeda K. Dental root resorption and repair: histology and histometry during physiological drift of rat molars. *J Periodontal Res* 2003;38(5):525-32.
30. Sheehan DC, Hrapchak BB. *Theory and practice of histotechnology*. 2d ed. St. Louis: Mosby; 1980.
31. Brain EB. *The preparation of decalcified sections*. Springfield, Ill: Charles C Thomas; 1967.
32. Rasband W. *ImageJ*. 1.43u ed. Bethesda, MD: US NIH; 2009.

33. Ho SP, Goodis H, Balooch M, Nonomura G, Marshall SJ, Marshall G. The effect of sample preparation technique on determination of structure and nanomechanical properties of human cementum hard tissue. *Biomaterials* 2004;25(19):4847-57.
34. ASTM. E384 - Standard Test Method for Knoop and Vickers Hardness of Materials. West Conshohocken, PA: American Standard for Testing Materials International. p. 399.
35. Bosshardt DD, Schroeder HE. Cementogenesis reviewed: a comparison between human premolars and rodent molars. *Anat Rec* 1996;245(2):267-92.
36. Liu ZJ, Ikeda K, Harada S, Kasahara Y, Ito G. Functional properties of jaw and tongue muscles in rats fed a liquid diet after being weaned. *J Dent Res* 1998;77(2):366-76.
37. Sako N, Okamoto K, Mori T, Yamamoto T. The hardness of food plays an important role in food selection behavior in rats. *Behav Brain Res* 2002;133(2):377-82.
38. Hoffman MM. Quantitative studies in the development of the rat molar. *American Journal of Orthodontics* 1940(26):854-74.
39. Lasfargues JJ, Saffar JL. Effects of prostaglandin inhibition on the bone activities associated with the spontaneous drift of molar teeth in the rat. *Anat Rec* 1992;234(3):310-6.
40. Kraw AGaE, D.H. Continuous attachment of the periodontal membrane. *American Journal of Anatomy* 1967;120(1):133-47.
41. Vignery A, Baron R. Dynamic histomorphometry of alveolar bone remodeling in the adult rat. *Anat Rec* 1980;196(2):191-200.

42. Ho SP, Kurylo MP, Fong TK, Lee SS, Wagner HD, Ryder MI, et al. The biomechanical characteristics of the bone-periodontal ligament-cementum complex. *Biomaterials* 2010;31(25):6635-46.
43. Berkovitz BKB, Moxham BJ, Newman HN. *The Periodontal ligament in health and disease*. 1st ed. Oxford ; New York: Pergamon Press; 1982.
44. Rippin JW. Collagen turnover in the periodontal ligament under normal and altered functional forces. I. Young rat molars. *J Periodontal Res* 1976;11(2):101-7.
45. Kaneko S, Ohashi K, Soma K, Yanagishita M. Occlusal hypofunction causes changes of proteoglycan content in the rat periodontal ligament. *J Periodontal Res* 2001;36(1):9-17.
46. Amemiya A. An electron microscopic study on the effects of extraction of opposed teeth on the periodontal ligament in rats. *Jpn J Oral Biol* 1980(22):72-83.
47. Cohn SA. Disuse atrophy of the periodontium in mice. *Arch Oral Biol* 1965;10(6):909-19.
48. Gianelly AAaG, H.M. *Biologic basis of orthodontics*. Philadelphia: Lea & Febiger; 1971.
49. Inoue M. Histological studies on the root-cementum of the rat molars under hypofunctional condition. *J Jpn Prosthodont Soc* 1961(5):29-34.
50. Kinoshita Y, Tonooka K, Chiba M. The effect of hypofunction on the mechanical properties of the periodontium in the rat mandibular first molar. *Arch Oral Biol* 1982;27(10):881-5.
51. Koike K. The effects of loss and restoration of occlusal function on the periodontal tissues of rat molar teeth: histopathological and histometrical investigation. *J Jpn Soc Periodont* 1996(38):1-19.

52. Kronfeld R. Histologic study of the influence of function on the human periodontal membrane. *J Am Dent Assoc* 1931(18):1242-74.
53. Saeki M. Experimental disuse atrophy and its repairing process in the periodontium of rat molar. *J Stomatol Soc Jpn* 1959(26):317-47.
54. McCulloch CA, Lekic P, McKee MD. Role of physical forces in regulating the form and function of the periodontal ligament. *Periodontol 2000* 2000;24:56-72.
55. Robling AG, Castillo AB, Turner CH. Biomechanical and molecular regulation of bone remodeling. *Annu Rev Biomed Eng* 2006;8:455-98.
56. Junqueira LC, Bignolas G, Brentani RR. Picrosirius staining plus polarization microscopy, a specific method for collagen detection in tissue sections. *Histochem J* 1979;11(4):447-55.
57. Chattah NL. Design strategy of minipig molars using electronic speckle pattern interferometry: comparison of deformation under load between the tooth-mandible complex and the isolated tooth. *Adv Mater* 2008(20):1-6.
58. Ho SP, Balooch M, Marshall SJ, Marshall GW. Local properties of a functionally graded interphase between cementum and dentin. *J Biomed Mater Res A* 2004;70(3):480-9.
59. Marshall GW, Jr., Balooch M, Gallagher RR, Gansky SA, Marshall SJ. Mechanical properties of the dentinoenamel junction: AFM studies of nanohardness, elastic modulus, and fracture. *J Biomed Mater Res* 2001;54(1):87-95.
60. Zaslansky P, Friesem AA, Weiner S. Structure and mechanical properties of the soft zone separating bulk dentin and enamel in crowns of human teeth: insight into tooth function. *J Struct Biol* 2006;153(2):188-99.
61. Frost HM. Bone remodelling dynamics. Springfield, Ill.,: Thomas; 1963.

62. Frost HM. Bone modeling and skeletal modeling errors. Springfield, Ill.,: Thomas; 1973.
63. Frost HM. Intermediary organization of the skeleton. Boca Raton, Fla.: CRC Press; 1986.
64. Frost HM. Obesity, and bone strength and "mass": a tutorial based on insights from a new paradigm. *Bone* 1997;21(3):211-4.
65. Jee WS, Frost HM. Skeletal adaptations during growth. *Triangle* 1992;31(2/3):77-88.
66. Roberts WE, Huja S, Roberts JA. Bone modeling: biomechanics, molecular mechanisms, and clinical perspectives. *Seminars in orthodontics* 2004;10(2):123-61.
67. Balooch M, Habelitz S, Kinney JH, Marshall SJ, Marshall GW. Mechanical properties of mineralized collagen fibrils as influenced by demineralization. *J Struct Biol* 2008;162(3):404-10.
68. Gupta HS, Seto J, Wagermaier W, Zaslansky P, Boesecke P, Fratzl P. Cooperative deformation of mineral and collagen in bone at the nanoscale. *Proc Natl Acad Sci U S A* 2006;103(47):17741-6.

FIGURES

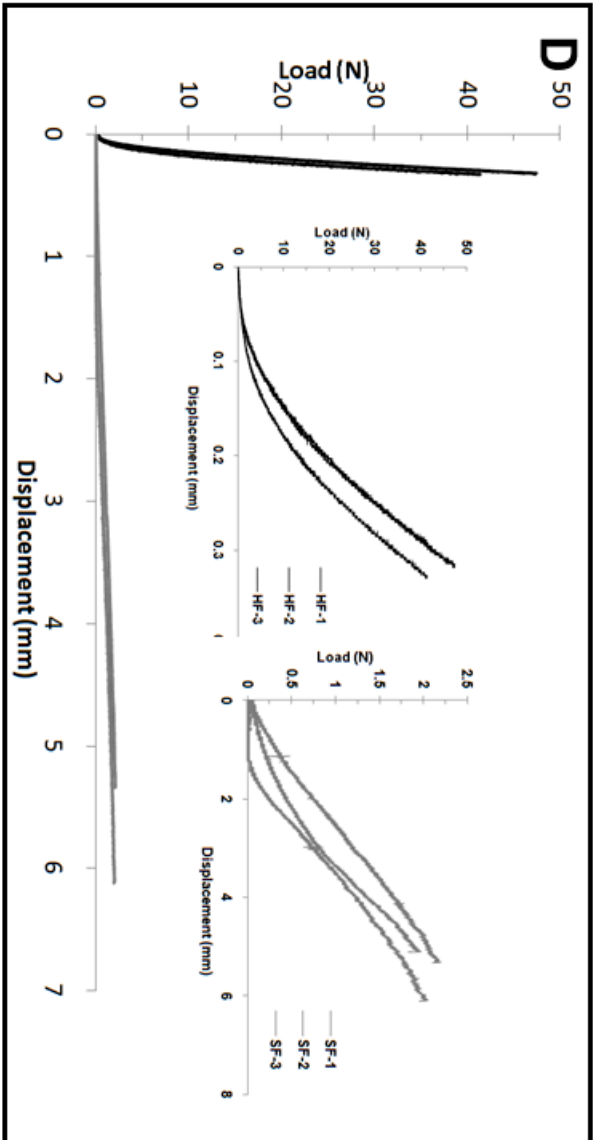
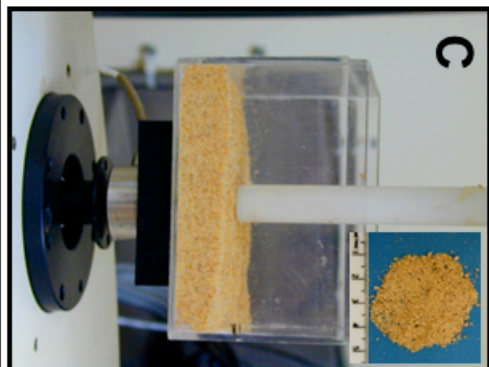
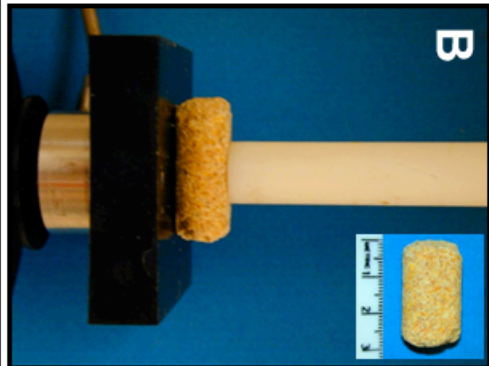


Figure 1. A) Compression testing system. B) Individual unconfined hard pellets were compressively loaded to determine hard food stiffness. C) Powdered soft food was confined within a hard plastic container and compressively loaded to determine soft food stiffness. D) Stiffness of the hard food (HF 1-3) and soft food (SF 1-3) was determined by the slope of the linear portion of the load versus the displacement curve. Mean stiffness of hard food: $150 \pm 15 \text{ N/mm}$. Mean stiffness of soft food: $0.4 \pm 0.1 \text{ N/mm}$.

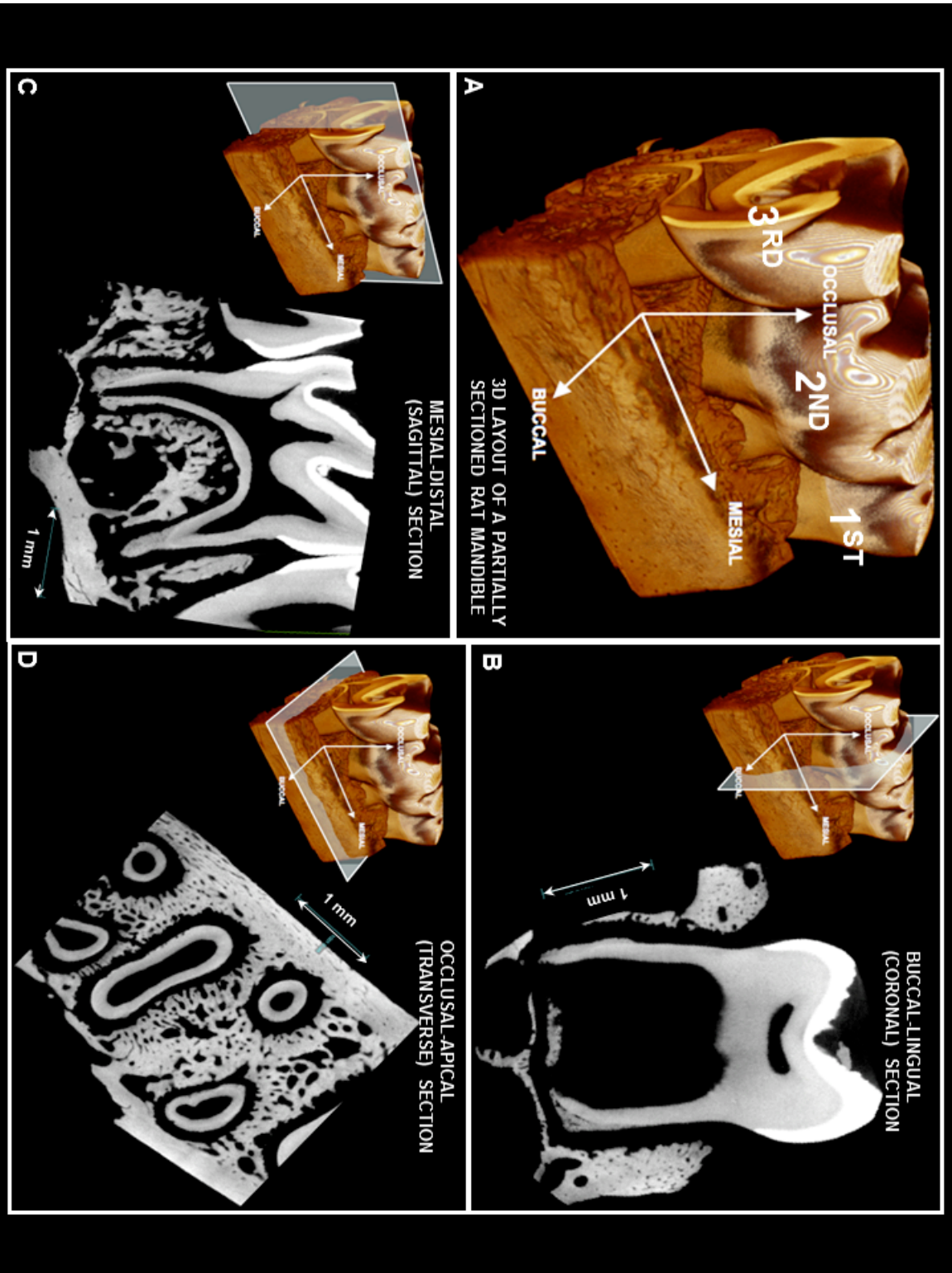


Figure 2. A) 3D reconstruction of mandibular molar region. B-D) Reconstructed 2D slices representing buccal-lingual, mesial-distal, and occusal-apical planes respectively.

Scale bar = 1mm

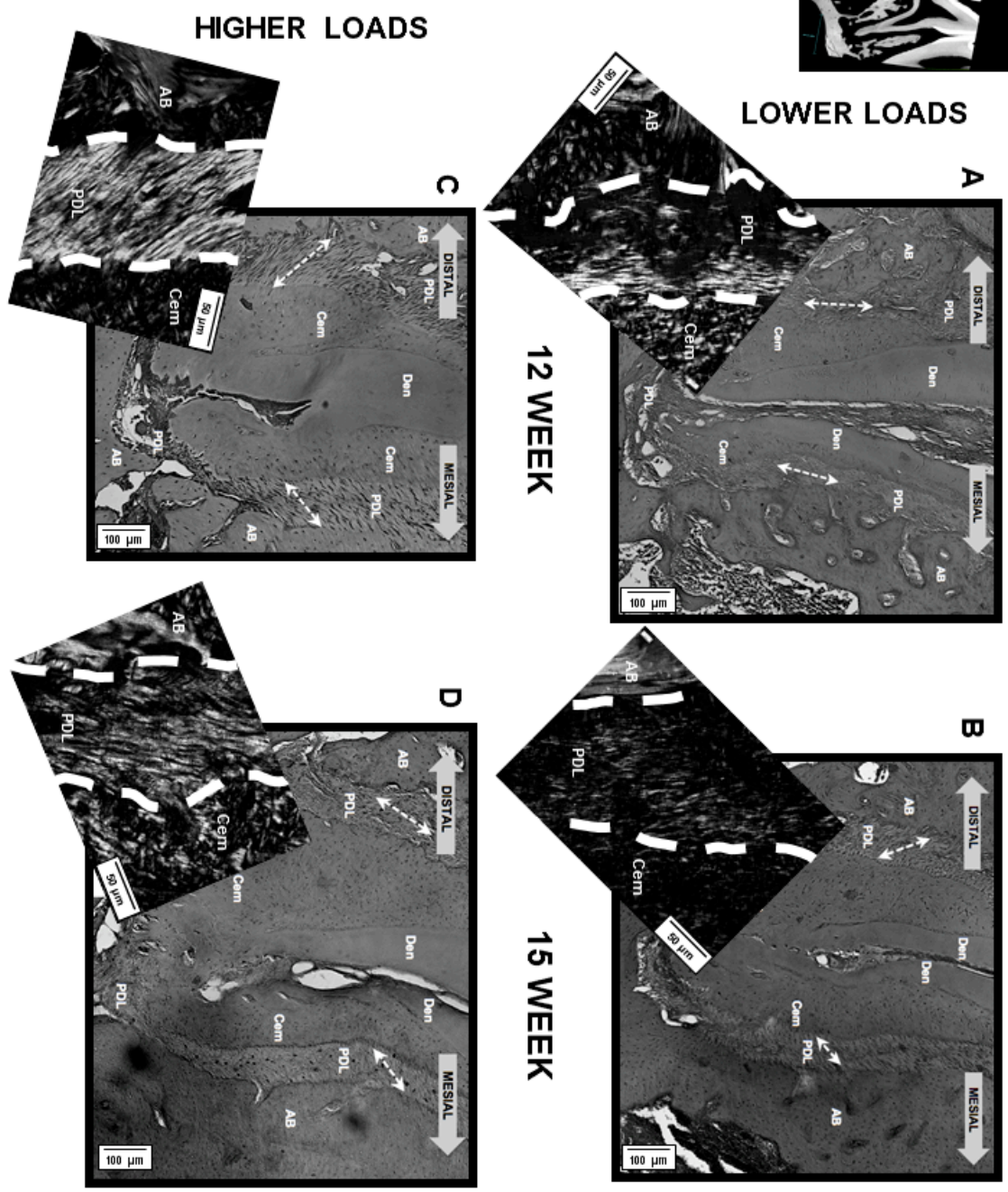


Figure 3. Light microscope images of M2 at 10x, stained with H&E to illustrate the variations in PDL orientation. Each inset is a polarized light image of a representative bone-PDL-cementum attachment site of M2/D at 40x , stained with Picrosirius Red for detection of collagen fiber birefringence. A,B) Lower loads may lead to less organized PDL collagen fibrils, resulting in a patchy, dim appearance of the PDL. C,D) Higher loads maintain well-organized healthy PDL collagen fibrils, resulting in a distinct, bright appearance of the PDL. AB = alveolar bone, Cem = cementum, Den = dentin, PDL = periodontal ligament. Scale bars = 100 μ m, inset scale bars = 50 μ m

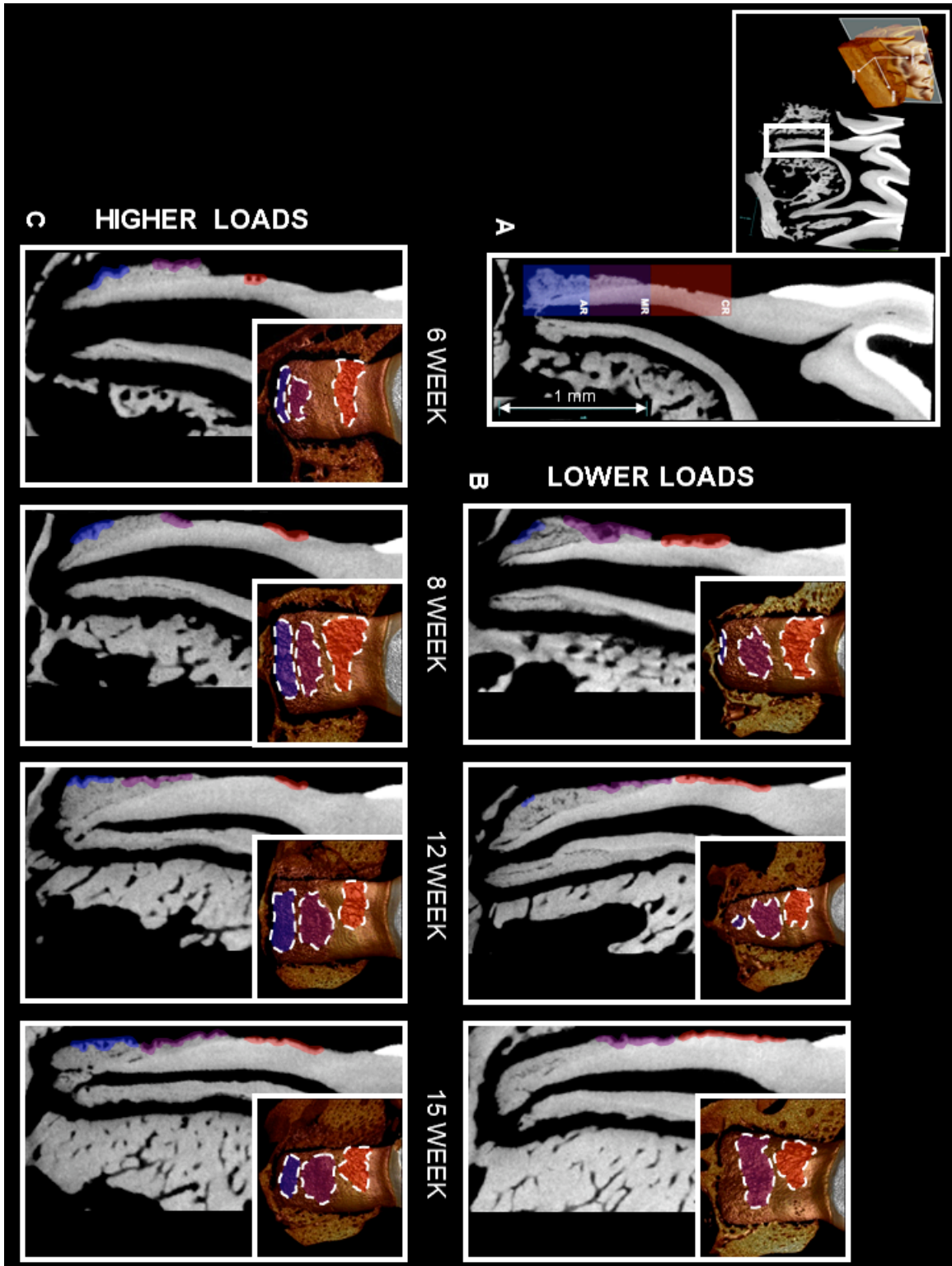


Figure 4. A) Diagram illustrating the observed regions of resorption on a representative mandibular second molar mesial-distal 2D slice: The coronal region (CR), all primary cementum, in red, the mid-root region (MR), spanning the interface of the primary and secondary cementum, in purple, and the apical region (AR), all secondary cementum, in blue. B,C) Areas of resorption were identified qualitatively, and colored according to region in both mesial-distal 2D reconstructed slices and corresponding 3D reconstructions for all groups. Extensive resorption can be observed in the CR and MR regions for all groups. However, in the lower functional load groups (B) there is little or no resorption in the AR region compared to the higher functional load groups (C).

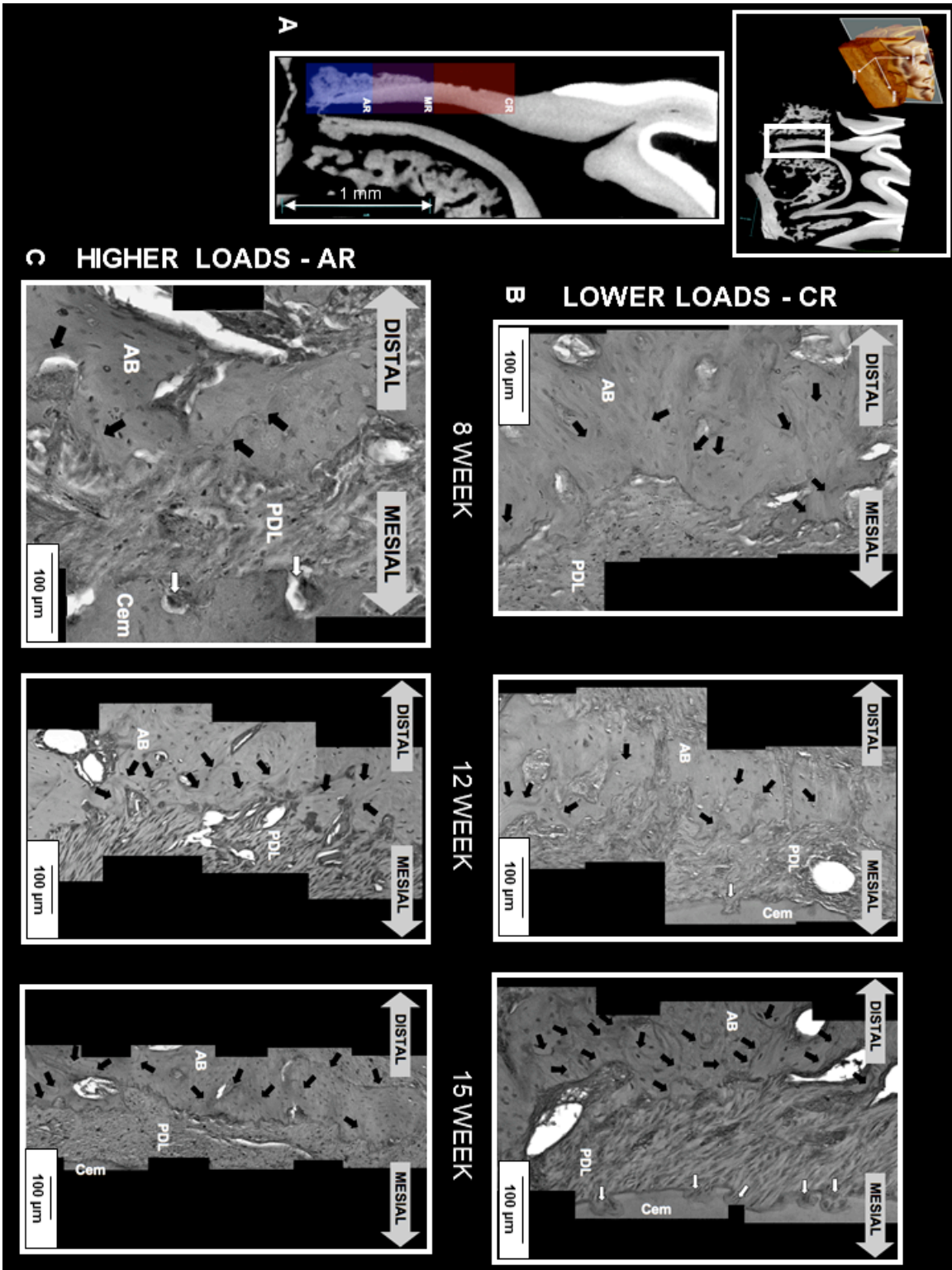
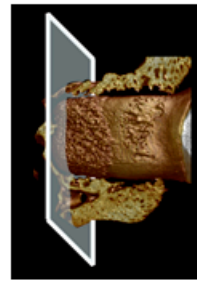
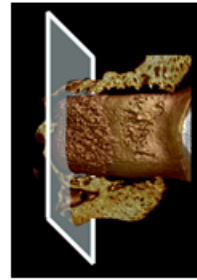


Figure 5. A) Diagram illustrating the observed regions of resorption on a representative mandibular second molar mesial-distal 2D slice: The coronal region (CR), all primary cementum, in red, the mid-root region (MR), spanning the interface of the primary and secondary cementum, in purple, and the apical region (AR), all secondary cementum, in blue. B,C) Light microscope images of M2/D at 20x, stained with H&E to illustrate the variations in cement lines in alveolar bone. B) Cement lines (black arrows) increase with age, especially in the CR region opposing areas of primary cementum resorption (white arrows). C) Cement lines (black arrows) increase with age, especially in the AR region opposing areas of secondary cementum resorption (white arrows). AB = alveolar bone, Cem = cementum, PDL = periodontal ligament. Scale bars = 100 μ m

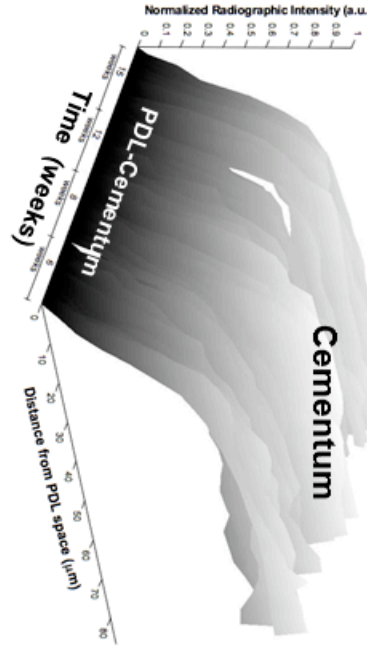
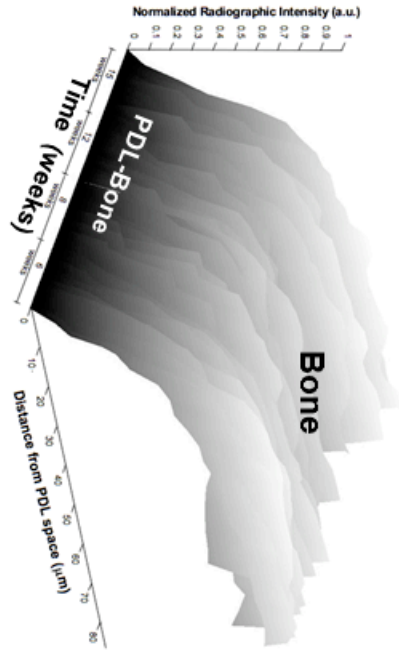


ALVEOLAR BONE
APICAL



CEMENTUM
APICAL

LOWER LOADS



HIGHER LOADS

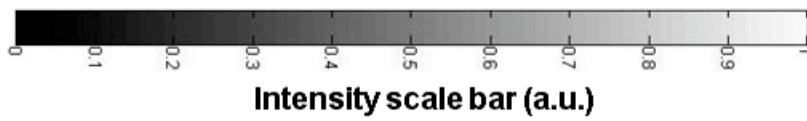
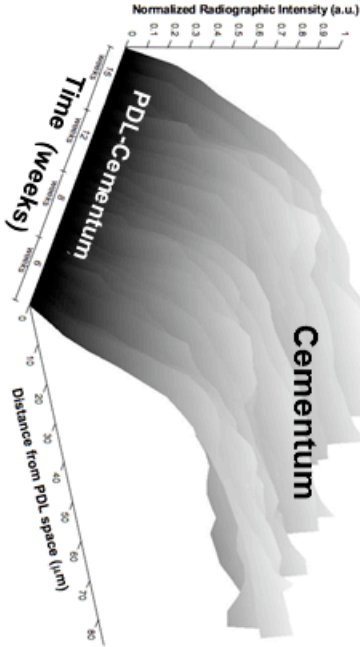
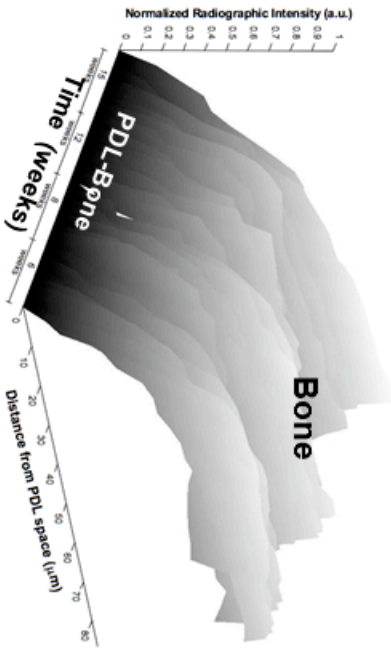


Figure 6. Intensity gradient (normalized) due to X-ray attenuation in alveolar bone near the bone-PDL interface for both higher and lower functional load groups at all time points, and in the secondary cementum near the cementum-PDL interface for both higher and lower functional load groups at all time points in the apical region (secondary cementum is localized to the apical 1/3 of the root). The 6 week higher load group data was duplicated in the lower load plot for ease of comparison. For all time points and locations, the intensity sharply increases in the first 25 μ m from the PDL space, corresponding to a mineralization gradient at this interface. However, there were no statistically significant differences between the higher and lower load groups.

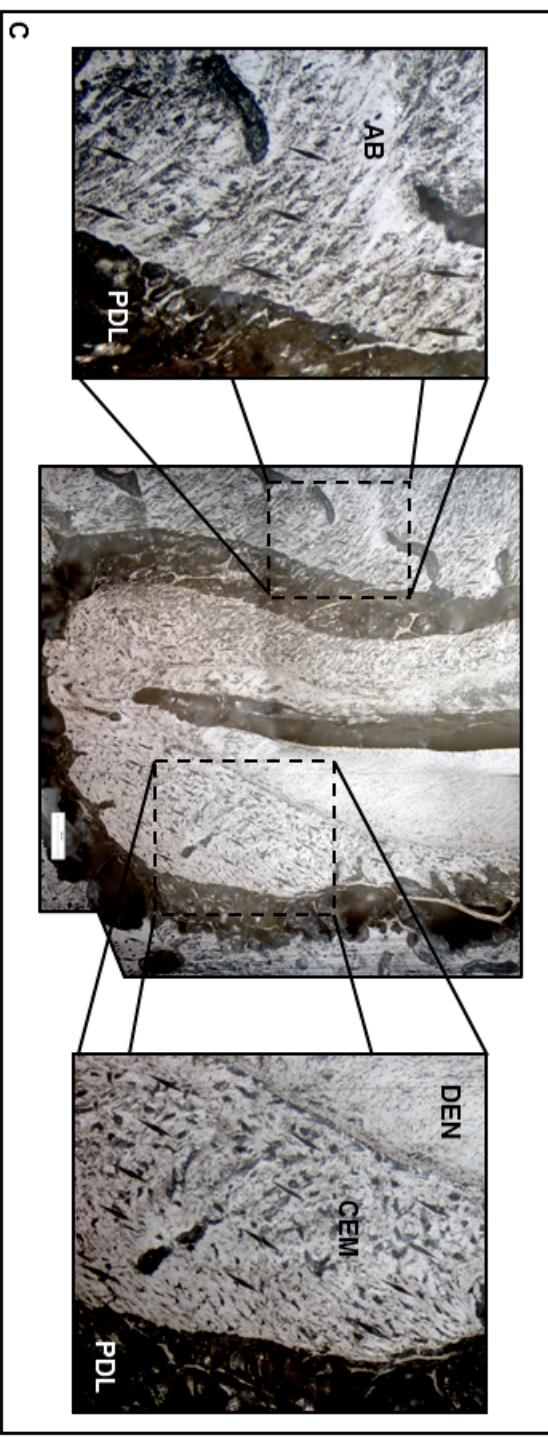
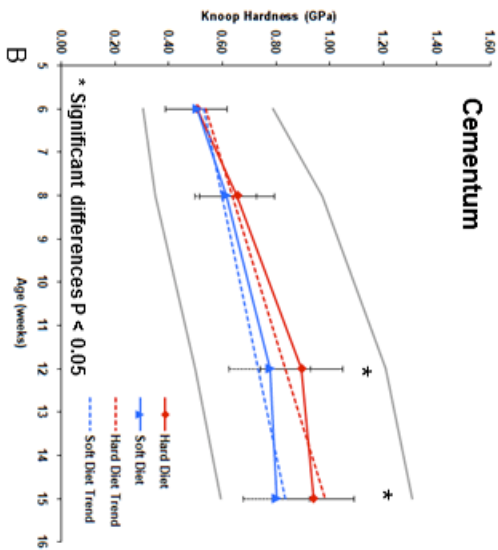
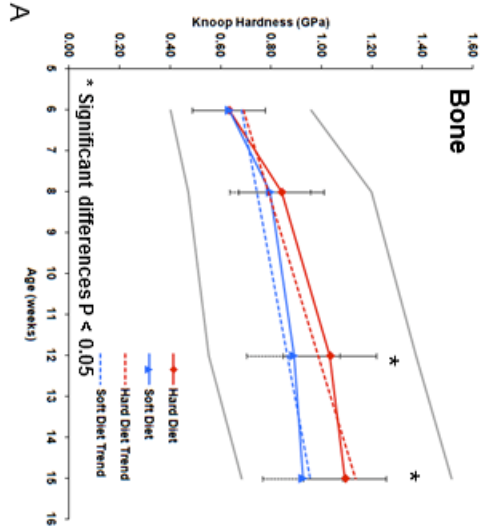


Figure 7. A) Mean hardness values of alveolar bone determined by microindentation for higher load and lower load groups at each time point. Range of hardness values are represented by gray lines above (maximum) and below (minimum). At all experimental time points (8, 12, and 15 weeks) bone hardness in the higher load group was greater than in the lower load group. Asterisks indicate statistical significance ($p < 0.05$) between groups at the 12 and 15 week time points. B) Mean hardness values of secondary cementum determined by microindentation for higher load and lower load groups at each time point. Range of hardness values are represented by gray lines above (maximum) and below (minimum). At all experimental time points (8, 12, and 15 weeks) cementum hardness in the higher load group was greater than in the lower load group. Asterisks indicate statistical significance ($p < 0.05$) between groups at the 12 and 15 week time points. C) Light microscope images illustrate microindents in alveolar bone (AB) and secondary cementum (CEM). PDL = Periodontal Ligament, DEN = Dentin. Scale bar = $100\mu\text{m}$

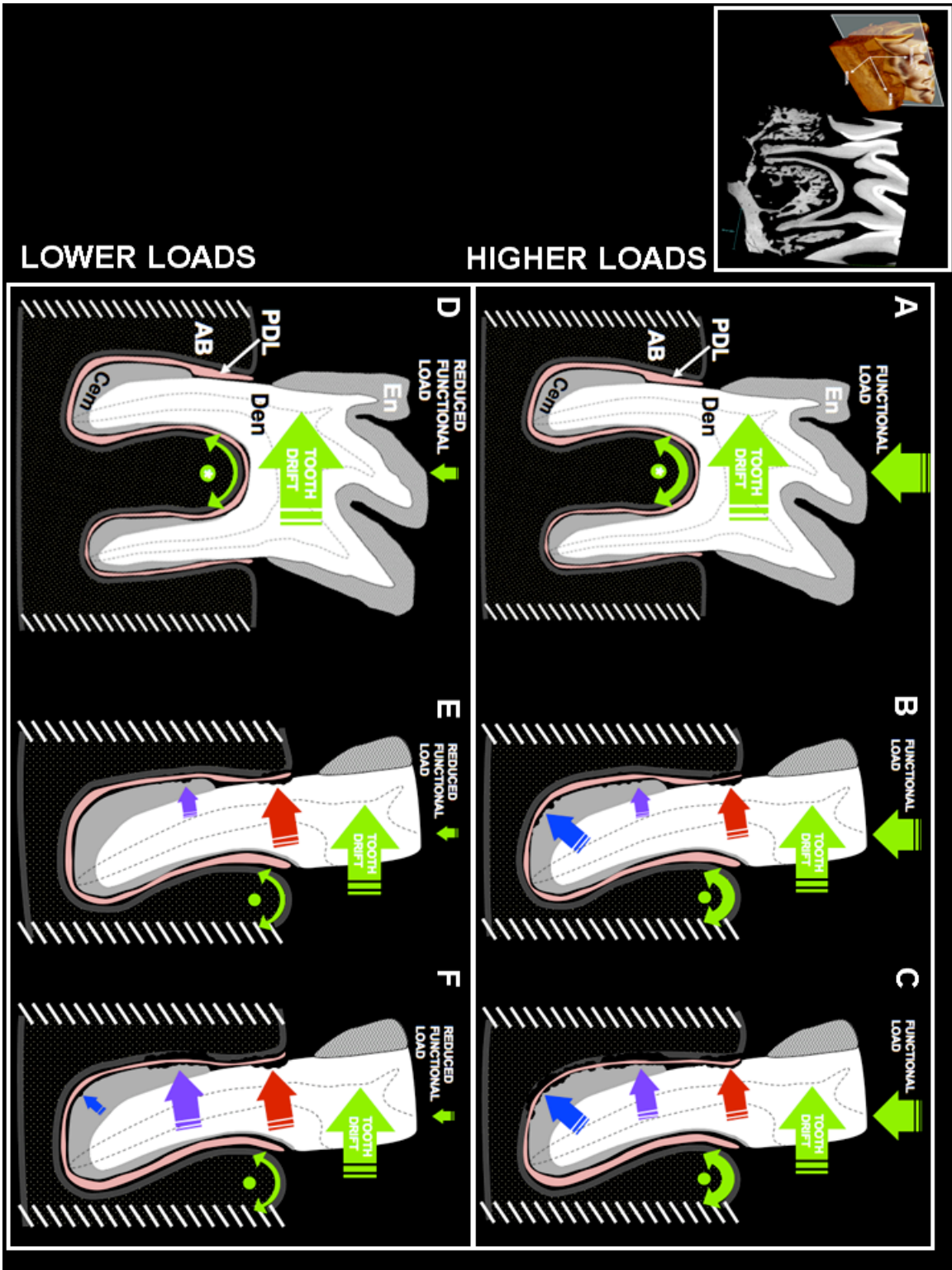
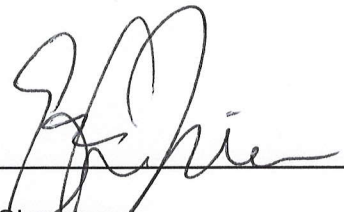


Figure 8. Schematic diagram of the directional forces acting on the second mandibular rat molar and a model for the load-mediated adaptation of the hard and soft tissues. A) The hard pellet diet provides a high functional load and apically directed forces in addition to the distally directed forces of tooth drift. Together, these forces also cause the tooth to rotate, with the inter-radicular bone as the fulcrum point (*). B) The rotation redirects the apical and distal forces, causing regional PDL compression between the alveolar bone and the tooth and resulting in resorption in the coronal, midroot, and apical regions. C) Continued function results in combined rotational, apical, and distal forces, causing compression of the PDL, resorption, and a combined tipping and translating movement of the tooth. D) The soft, powdered diet decreases the functional load, so that the distally directed forces of tooth drift dictate tooth movement. The anatomy of the inter-radicular bone also creates a fulcrum point (*) around which some rotational movement is seen. E) The distal tooth drift together with some rotation causes regional PDL compression between the alveolar bone and the coronal portion of the tooth, resulting in resorption. F) In the absence of substantive functional loading, the rotational force on the tooth is minimized, and little compressive force acts on the apical portion of the root. Meanwhile, subsequent tooth drift acts to translate the tooth distally, causing regional PDL compression between the alveolar bone and the tooth in the coronal and midroot regions. En = Enamel, Den = Dentin, Cem = Secondary Cementum, PDL = Periodontal Ligament, AB = Alveolar Bone.

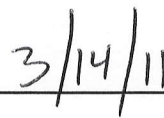
PUBLISHING AGREEMENT

It is the policy of the University to encourage the distribution of all theses, dissertations, and manuscripts. Copies of all UCSF theses, dissertations, and manuscripts will be routed to the library via the Graduate Division. The library will make all theses, dissertations, and manuscripts accessible to the public and will preserve these to the best of their abilities, in perpetuity.

I hereby grant permission to the Graduate Division of the University of California, San Francisco to release copies of my thesis, dissertation, or manuscript to the Campus Library to provide access and preservation, in whole or in part, in perpetuity.



Author Signature



Date